ChemComm

Accepted Manuscript

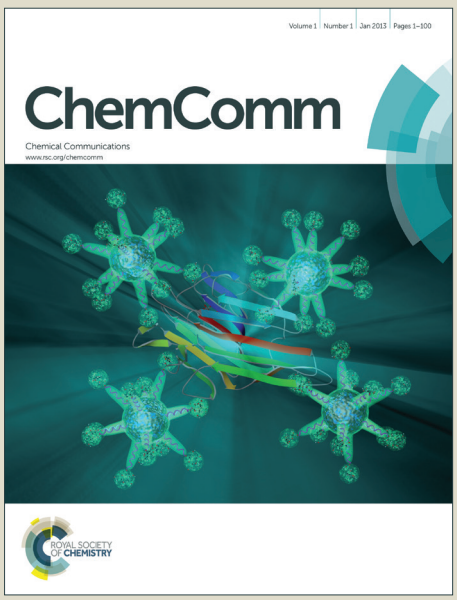

ROYAL SOCIETY OF CHEMISTRY

www.rsc.org/chemcomm

Chemical Communications

RSCPublishing

COMMUNICATION

Plasmon-assisted and visible-light induced graphene oxide reduction and efficient fluorescence quenching

Cite this: DOI: 10.1039/x0xx00000x

Dinesh Kumar[a], Sandeep Kaur[a], and Dong-Kwon Lim[a,*]

Received 00th January 2013,
Accepted 00th January 2013

DOI: 10.1039/x0xx00000x

www.rsc.org/

Here we report new and efficient synthetic method of reduced graphene oxide using visible-light and plasmonic nanoparticles at room temperature. The r-GO prepared using visible light showed excellent fluorescence quenching properties and target detection capabilities.

Due to the unique physical properties of graphene,[1] it has been investigated for wide ranges of potential applications such as nanoelectronics,[2] energy storage materials,[3] polymer composite materials,[4] biosensing, and drug delivery.[5] Chemical vapor deposition is one of efficient method to produce pristine state of graphene layer on the substrate, but for the application of graphene in bio science chemical reduction method in solution is the best way to obtain colloidal state of reduced graphene oxide (r-GO). Graphite has been used for the preparation of graphene oxide (GO) which in turn is widely used as precursor for the synthesis of r-GO.[6] The exfoliated planes of GO are decorated with hydroxyl and epoxide groups, while the edges contain carbonyl and carboxylic groups. These oxygen functionalities increases the hydrophilic character of GO and improves its water solubility by destroying the aromaticity of the graphene framework. To recover its physical properties, reduction of hydroxyl, epoxide, and carbonyl groups in GO are essential.[7]

The reduction of GO was mostly carried out with hydrazine or its derivatives[4,8,9] or by thermal treatment (550 – 1,100 °C) in inert or reducing atmosphere.[10,11] These processes required the use of toxic chemicals, time consuming reactions, and increased energy demand for the process.[12,13,14] Photo-irradiating reduction processes to produce reduced graphene oxide (r-GO) have also been reported. UV-induced,[15,16,17] photo-thermal reduction using a pulsed xenon flash,[18] pulsed laser,[19] and photo-thermal heating of camera flash lights were reported.[20] Because of low conversion efficiency of photo-induced method, UV or pulsed laser that can deliver high photon energy has been widely applied. Due to the low photon energy of visible light, it was not popular light source for r-GO synthesis. The use of plasmonic nanoparticle would be one way to overcome the current drawbacks of visible light. The use of silver nanoparticle with electron donor to reduce GO into r-GO was reported.[21] But the systemic studies with wide ranges of plasmonic nanostructures made of gold have not been investigated in detail. The photocatalytic reduction of GO is useful synthetic method since it can minimize the use of toxic chemicals and it can also improve the current understanding of hot-electron based photocatalytic effect of plasmonic nanoparticle.[22]

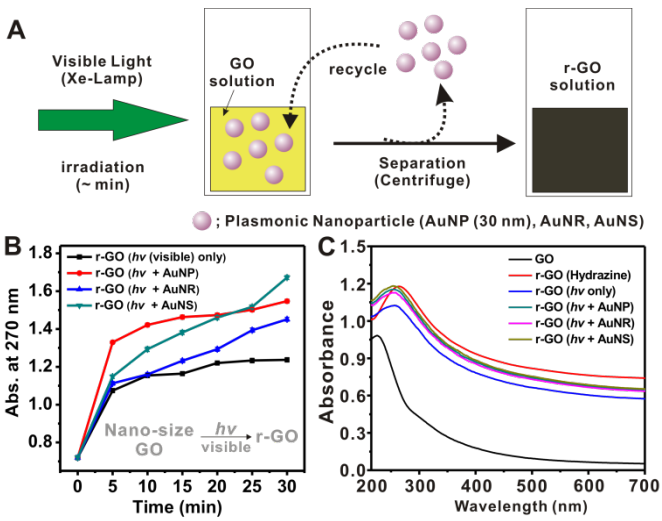

Fig. 1 (A) Schematic description of plasmon assisted and visible light induced GO reduction, (B) the reaction progress monitored at 270 nm with visible light (400 – 780 nm) and nano-sized GO solution without nanoparticle or with AuNP, AuNR, and AuNS, (C) UV-Vis spectrum of GO and r-GO obtained from chemical (hydrazine) method or light-induced method.

In this study, we report an efficient photocatalytic reduction of GO using visible light and plasmonic nanoparticles. We found the reaction progress was strongly dependent on the structures of plasmonic nanoparticles such as spherical gold nanoparticle (AuNP), gold nanorod (AuNR), and gold nanostar (AuNS). The quality of reduced GO prepared using visible light and plasmonic nanoparticles

was as excellent as that of chemical reduced GO, which was demonstrated by a series of analysis and fluorescence quenching based DNA detection scheme.

First, micro-sized GO solution (average particle size = 709 nm, **Fig. S1**) was prepared by following modified Hummer's method.[23] Micro-sized GO was extensively sonicated for 2 hrs, followed by 2 times centrifugation at 12,000 rpm (15 min) in order to obtain nano sized GO solution by discarding precipitates (average particle size = 87 nm, **Fig. S1**). The reduction of GO was performed with Xe lamp (Ceramax®, Waltham, USA) for visible light (400 – 780 nm) source (**Fig. S2**) or near-infrared (NIR) laser (808 nm). The reduction of GO was carried out with or without plasmonic nanoparticles at room temperature. Purchased spherical AuNP (30 nm) (Tedpella. Radding CA) was used, CTAB-AuNR[24] (Aspect ratio; 3.5, λ_{max} = 730 nm) and AuNS (30 nm, λ_{max} = 740 nm) were prepared (see method for synthetic details).[25] For photocatalytic reduction of GO, 10 mL of GO solution (OD 1.0 at 230 nm, 0.125 mg/ml) containing 1 ml of gold nanoparticles (Abs 1.0 at 520 nm or 730 nm or 740 nm, respectively (**Fig. S3**)) and 100 μL of ammonium hydroxide (28%, w/v %) were placed in pyrex glass reactor equipped with water-circulating jacket (**Fig. S4**), irradiated with Xe lamp with the power density of 1.56 W/cm^2 for 30 min. After illumination for 30 min, solutions were centrifuged to remove gold nanoparticles (**Fig. 1A & S5**). It should be noted that the nanosized GO is not possible to centrifuge down in moderate ranges of rpm (5,000 ~ 12,000), which facilitate the selective separation of r-GO from reaction mixture (**Fig. S5**). The shift in UV spectra from 230 nm to 270 nm indicate the formation of r-GO, we monitored the absorbance changes at 270 nm at every 5 min (**Fig. 1B**). To minimize the possibility of thermal reduction, the temperature of reaction mixture was maintained at 25 °C by circulating water into water circulating jacket (**Fig. S4**).

When visible light was irradiated into GO solution without gold nanoparticle, it showed gradual absorbance changes from 0.7 to 1.2 (black line). But the same reactions with AuNP (red line), AuNR (black line), and AuNS (green line) showed higher absorption (from 0.7 to 1.5, 1.4, 1.6, respectively) at 270 nm as shown in **Fig. 1B**. Interestingly, the use of AuNP showed the highest absorbance at 270 nm until 20 min of reaction time than AuNR or AuNS. But after 20 min, the reaction with AuNS showed rapid increase of absorbance at 270 nm. The solution color was changed from light yellow-brown to black color within few minutes (**Fig. S6**). The UV-Vis spectra showed red shifted peak from ~ 230 nm to ~ 270 nm indicating the conversion of GO into r-GO. The UV-Vis spectra of r-GO (chemically reduced) clearly showed the distinguished absorbance at 270 nm and broad absorption spectrum in the visible and NIR regions (red line in **Fig. 1C**). The r-GO solution produced with visible light also showed absorbance around 270 nm and broad absorption in visible region. As a whole, light-induced r-GO solution showed lower absorption properties in the visible and NIR regions (**Fig. 1C**).

The nanostructure-dependent reaction progress observed in **Fig. 1A** indicates the role of plasmonic nanoparticle in GO reduction. The absorption band of AuNP was 520 nm, while the absorption of AuNR and AuNS were in the ranges of 700 and 800 nm (**Fig. S3**). AuNP can absorb higher region of light energy in the visible, which subsequently induce higher photocatalytic activity than that of AuNR or AuNS. The sudden increase of absorbance after 25 min observed in the case of AuNS was found to be the changed plasmonic nanostructures. As shown in **Fig. 2A**, AuNP and AuNR showed no noticeable changes of nanostructures before and after light illumination, but the structure of AuNS was changed into spherical nanoparticles, which lead to the increased catalytic properties as AuNP does. The UV-Vis spectra of AuNS solution were also significantly blue shifted, indicating the changes of nanostructure from star-shape to spherical shape (**Fig. 2B**).

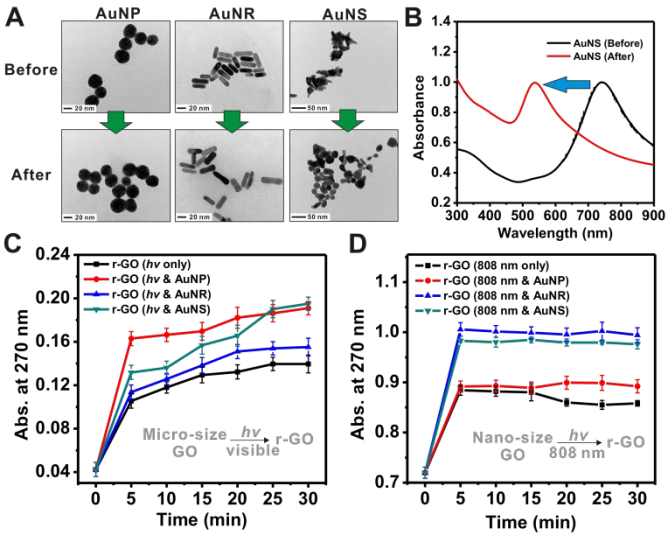

Fig. 2 (A) TEM images of AuNP, AuNR, and AuNS before and after the GO reduction, (**B**) UV-Vis spectra of AuNS before and after the GO reduction, (**C**) the reaction progress of micro-size GO with visible light and plasmonic nanoparticles, (**D**) the reaction progress of nano-sized GO with NIR light (808 nm) and plasmonic nanoparticles.

Furthermore, we investigated the size effect of GO sheet in this reaction by performing reaction using micro-sized GO sheet solution (**Fig 2C**). Exactly same trends of plasmon effect were observed (AuNP shows higher absorption at 270 nm than that of AuNR or AuNS), but the reactions with micro-sized GO showed very small changes of optical density (ΔOD = 0.15 in case AuNS), which is significantly lower than that of nano-sized GO (ΔOD = 0.9 in case AuNS).

We also investigated wavelength dependence by performing the reactions with NIR laser (808 nm, power density: 0.36 W/cm^2) for the nano-sized GO reduction in order to understand the contributions of plasmonic nanoparticles (**Fig. 2D**). The reaction showed almost steady-state after 5 min illuminations, AuNR and AuNS showed higher reaction progress than AuNP or the reactions without using plasmonic nanoparticles. These results are well-matched with plasmonic absorption band of AuNR and AuNS and wavelength of incident light. Therefore, we can conclude the reduction with visible light can be significantly expedited by use of plasmonic nanoparticles. Importantly, the recycled AuNP also showed the efficient conversion of GO into r-GO as shown in **Fig. S7**, which is one of important factors to be a cost effective r-GO synthetic method.

Next, to evaluate the quality of r-GO produced from visible light, we performed a series of spectroscopic analysis such as Raman, XRD, SEM, FT-IR, and XPS. We also performed fluorescence quenching based DNA detection experiment to confirm the

potentials of applications of visible-light induced r-GO. The Raman spectrum of GO and r-GO obtained from chemically or light-induced method was displayed in **Fig. 3A**. In Raman spectrum of GO, the D band corresponding to edge planes and disordered structures and the G band corresponding to ordered sp^2 bonded carbon were appeared at 1,327 cm^{-1}, 1,590 cm^{-1}, respectively.[26,27] The Raman spectrum of the chemically reduced GO, visible light irradiated GO and plasmon assisted GO reduction under visible light also shows the presence of D and G bands at 1,336 and 1,592 cm^{-1}, respectively. The D/G intensity ratio (I_D/I_G) of GO and r-GO produced chemically or light-induced without or with NP (AuNR, AuNP, and AuNS) were 1.03, 1.13, 1.12, 1.13, 1.13 and 1.13, respectively. The analysis of X-ray diffraction also showed successful formation of r-GO, since the characteristic peak (002) of graphite at 26.48° disappeared in GO and the peak (001) at 10.21° corresponding to GO was also completely disappeared as show in **Fig. 3B**. The surface morphology of GO and r-GO were examined by use of FE-SEM (Hitachi SU-70, Tokyo, Japan). **Fig. 3C-a** exhibits the thin folded sheet structure of GO and **Fig. 3C (b-f)** shows the randomly aggregated disordered solids with crumpled sheets of r-GO produced by chemical method, light only, light & AuNP, light & AuNR and light & AuNS, respectively. Whereas, the r-GO produced by chemical method shows more braked, aggregated, and disordered sheets which was due to the use of harsh reaction conditions and chemicals (**Fig. 3C-b**). FT-IR analysis showed more detail of molecular structure information of r-GO (**Fig. S6**). The FT-IR spectrum of GO exhibits the presence of C=O (1,741 cm^{-1}), O–H (1,424 cm^{-1}), C=C (1,622 cm^{-1}), and C–O (1,070 cm^{-1}). After reduction of GO, the characteristic absorption bands of oxygen-containing groups (O–H, C=O, and C–O) were disappeared indicating that GO has been reduced to r-GO.

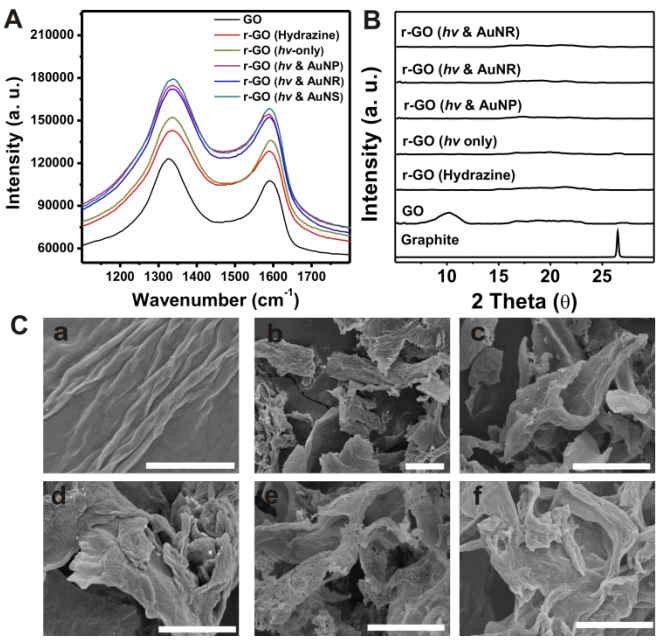

Fig. 3 (**A**) Raman spectra, (**B**) XRD data of GO and r-GO produced with chemical method and light-induced method without or with AuNP, AuNR, and AuNS, (**C**) representative FE-SEM images of (a) GO, (b) r-GO (chemical method), (c) r-GO (light only), (d) r-GO (light & AuNP), (e) r-GO (light & AuNR) and (f) r-GO (light & AuNS). (Scale bar = 5 µm).

Again, the XPS analysis also showed successful conversion of GO into r-GO, the C/O ratio of GO, r-GO (hydrazine), r-GO (*hv* only), and r-GO (*hv* + AuNP) were calculated to be 1.95, 4.81, 3.74, and 5.19, respectively, indicating the benefits of using plasmonic nanoparticles in the visible-light induced method (**Fig. S8**).

Due to the presence of sp^2 domains, r-GO showed excellent fluorescence quenching effect compare to GO, which is useful properties for biosensing applications such as detecting target DNA with multiplexing capability.[28] We used quenching properties of r-GO for fluorescent molecules in the single-stranded DNA and fluorescence recovery in the presence of target DNA to evaluate the quality of r-GO prepared using visible light and plasmonic nanoparticles (**Fig. 4**).

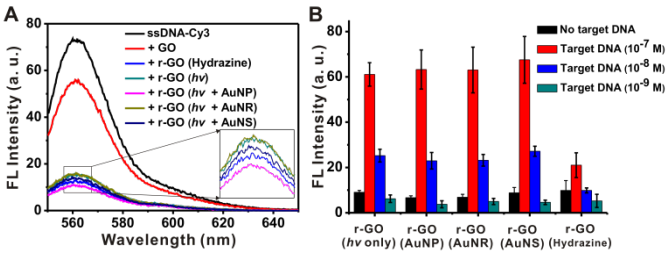

Fig. 4 (**A**) Fluorescence quenching of ssDNA-Cy3 using GO and r-GO chemically reduced or produced with visible light and plasmonic nanoparticle, (**B**) fluorescence recovery with varying concentration of target DNA (10^{-7} M, 10^{-8} M and 10^{-9} M).

For fluorescence quenching study of GO and various r-GO (chemically reduced, or light-induced with or without gold nanoparticle), 25 µL of graphene solution (OD 1.0 at 230 nm)) were incubated with 20 µL of ssDNA-Cy3 (10^{-6}M, (5'-ATC CTT ATC AAT ATT TAA CAA TAA TCC CTC-Cy3-3') and 1,955 µl of 0.3 M PBS (**Fig. 4A**). GO solution (red line) showed very little quenching effect, but the r-GO (magenta line) prepared by the use of AuNP with visible light showed excellent quenching effect as same as the chemically reduced r-GO (blue line) (**Fig. 4A**). This result shows the quality of visible light induced r-GO is excellent to be used for biosensing applications. Furthermore, in order to study the capability of fluorescence recovery, 200 µl of varying concentration (10^{-6} M, 10^{-7} M and 10^{-8} M) of complementary target DNA (5'-GAGGGATTATTGTTAAATATTGATAAGGAT-3') was incubated with 20 µl of 10^{-6} M (ssDNA-Cy3), 25µl of r-GO, and 1,755 µl of 0.3 M PBS. Interestingly, r-GO prepared by visible light and plasmonic nanoparticle showed good fluorescence recovery with the target DNA as compared to the chemically reduced GO (**Figs. 4B & S9**). The lesser ability of chemically reduced GO to recover target DNA could be due to the structural differences between light induced r-GO and chemically reduced r-GO. As can be seen in FT-IR analysis, there was more elimination of O-H groups in chemically reduced GO as compared to other light irradiated GO. Therefore, two possible reasons are expected in these results. One is stronger interactions between ssDNA-Cy3 and chemically reduced r-GO, another reason is the interactions between target DNA and basal plane of r-GO, both can result in the decreased amount of released ssDNA-Cy3 in solution.[28,29,30,31,32,33,34,35,36,37]

In conclusion, the use of visible light with plasmonic nanoparticle are possible to be an efficient synthetic method to produce r-GO, which is simple, chemical free, and energy efficient method. The successful preparation of r-GO was supported by various analytical

techniques such as UV-Vis spectroscopy, Raman, powder XRD, FT-IR, FE-SEM, and XPS. The r-GO prepared by light irradiation shows excellent quenching property over the fluorescence molecules modified on ssDNA and excellent fluorescence recovery, which is useful property for biosensing applications.[38] Since the current results were obtained from at room temperature without electron donor, the reduction of graphene oxide was possible by the function of hot-electron transferred from plasmonic nanoparticle, which is well matched with previous reports.[22, 39,40]

This work was supported by the National Research Foundation of Korea and the Brain Korea 21 PLUS Project. This paper was supported by research funds of Chonbuk National University in 2012.

Notes and references

[a]*Department of BIN Fusion Technology, Chonbuk National University, 567 Baeckje-daero, Jeonju 561-756, South Korea. E-mail; dklim@jbnu.ac.kr; Tel: +82-63-270-4728*

†Electronic Supplementary Information (ESI) available: Detailed experimental procedures, additional UV-visible, TEM, and Raman data. See DOI: 10.1039/c000000x/

References:

1 A. K. Gein. and. K. S. Novoselov, *Nature Materials*, 2007, **6**, 183.
2 B. Li, X. Cao, H. G. Ong, J. W. Cheah, X. Zhou, Z. Yin, H. Li, J. Wang, F. Boey, W. Huang and H. Zhang, *Advanced Materials*, 2010, **22**, 3058.
3 J. T.-W. Wang, J. M. Ball, E. M. Barea, A. Abate, J. A. Alexander-Webber, J. Huang, M. Saliba, I. Mora-Sero, J. Bisquert, H. J. Snaith and R. J. Nicholas, *Nano Letters*, 2013, **14**, 724.
4 D. A. D. S. Stankovich, G. H. B. Dommett, K. M. Kohlhaas, E. J. Zimney, E. A. Stach, R. D. Piner, S. T. Nguyen and R. S. Ruoff, *Nature*, 2006, **442**, 282.
5 L. Kong, Z. Ren, S. Du, J. Wu and H. Fu, *Chemical Communications*, 2014, **50**, 4921.
6 D. Li and R. B. Kaner, *Science*, 2008, **320**, 1170.
7 Y. Zhou, Q. Bao, B. Varghese, L. A. L. Tang, C. K. Tan, C.-H. Sow and K. P. Loh, *Advanced Materials*, 2010, **22**, 67.
8 M. J. A. V. C. Tung, Y. Yang and R. B. Kaner, , *Nat. Nanotechnol.* , 2009, **4**, 25.
9 M.-j. Li, C.-m. Liu, Y.-b. Xie, H.-b. Cao, H. Zhao and Y. Zhang, *Carbon*, 2014, **66**, 302.
10 H. A. Becerril, J. Mao, Z. Liu, R. M. Stoltenberg, Z. Bao and Y. Chen, *ACS Nano*, 2008, **2**, 463.
11 X. Wang, L. Zhi and K. Müllen, *Nano Letters*, 2007, **8**, 323.
12 S. J. P. a. R. S. Ruoff, *Nat Nanotechnol* 2009, **4**, 217.
13 L. B. A. W. Gao, L. J. Ci and P. M. Ajayan, *Nat Chem* 2009, **1**, 403.
14 Y. K. S. Some, Y. Yoon, H. J. Yoo, S. Lee, Y. Park and H. Lee, *Scientific Reports*, 2013, **3**, 1929.
15 O. Akhavan and E. Ghaderi, *The Journal of Physical Chemistry C*, 2009, **113**, 20214.
16 L. Guardia, S. Villar-Rodil, J. I. Paredes, R. Rozada, A. Martínez-Alonso and J. M. D. Tascón, *Carbon*, 2012, **50**, 1014.
17 T. Wu, S. Liu, H. Li, L. Wang and X. Sun, *Journal of Nanoscience and Nanotechnology*, 2011, **11**, 10078.
18 L. J. Cote, R. Cruz-Silva and J. Huang, *Journal of the American Chemical Society*, 2009, **131**, 11027.
19 L. Huang, Y. Liu, L.-C. Ji, Y.-Q. Xie, T. Wang and W.-Z. Shi, *Carbon*, 2011, **49**, 2431.
20 S. Gilje, S. Dubin, A. Badakhshan, J. Farrar, S. A. Danczyk and R. B. Kaner, *Advanced Materials*, 2010, **22**, 419.
21 T. Wu, S. Liu, Y. Luo, W. Lu, L. Wang and X. Sun, *Nanoscale*, 2011, **3**, 2142.
22 Z. Fang, Z. Liu, Y. Wang, P. M. Ajayan, P. Nordlander and N. J. Halas, *Nano Letters*, 2012, **12**, 3808.
23 L. J. Cote, F. Kim and J. Huang, *Journal of the American Chemical Society*, 2008, **131**, 1043.
24 T. Ming, L. Zhao, H. Chen, K. C. Woo, J. Wang and H.-Q. Lin, *Nano Letters*, 2011, **11**, 2296.
25 J. Xie, J. Y. Lee and D. I. C. Wang, *Chemistry of Materials*, 2007, **19**, 2823.
26 A. C. Ferrari and J. Robertson, *Physical Review B*, 2000, **61**, 14095.
27 F. Tuinstra and J. L. Koenig, *The Journal of Chemical Physics*, 1970, **53**, 1126.
28 Q. B. K. P. Loh, G. Eda and M. Chhowalla, *Nat Chem*, 2010, **2**, 1015.
29 J. Kim, L. J. Cote, F. Kim and J. Huang, *Journal of the American Chemical Society*, 2009, **132**, 260.
30 H. Li and L. J. Rothberg, *Analytical Chemistry*, 2004, **76**, 5414.
31 Y.-W. Zhang, H.-L. Li and X.-P. Sun, *Chinese Journal of Analytical Chemistry*, 2011, **39**, 998.
32 H. Li and X. Sun, *Chemical Communications*, 2011, **47**, 2625.
33 H. Li, Y. Zhang, L. Wang, J. Tian and X. Sun, *Chemical Communications*, 2011, **47**, 961.
34 S. Liu, L. Wang, Y. Luo, J. Tian, H. Li and X. Sun, *Nanoscale*, 2011, **3**, 967.
35 Z. Yang and C. Zhang, *Biosensors and Bioelectronics*, 2011, **29**, 167.
36 L. Wang, Y. Zhang, J. Tian, H. Li and X. Sun, *Nucleic Acids Research*, 2011, **39**, e37.
37 H. Li, Y. Zhang, Y. Luo and X. Sun, *Small*, 2011, **7**, 1562.
38 C.-H. Lu, H.-H. Yang, C.-L. Zhu, X. Chen and G.-N. Chen, *Angewandte Chemie International Edition*, 2009, **48**, 4785.
39 Q. Bao and K. P. Loh, *ACS Nano*, 2012, **6**, 3677.
40 Z. Xiong, L. L. Zhang, J. Ma and X. S. Zhao, *Chemical Communications*, 2010, **46**, 6099.

The use of plasmonic nanoparticles accelerated visible-light induced reduction of graphene oxide at room temperature.